On the effective integration of manufacturability constraints within the multi-scale methodology for designing variable angle-tow laminates

Marco Montemurro*

Arts et Métiers ParisTech, I2M CNRS UMR 5295, F-33400 Talence, France.

Anita Catapano

Bordeaux INP, Université de Bordeaux, I2M CNRS UMR 5295, F-33400 Talence, France

Author for Correspondence:
Marco Montemurro, PhD,
Arts et Métiers ParisTech,
I2M CNRS UMR 5295,
F-33400 Talence, France,
tel: +33 55 68 45 422,
fax: +33 54 00 06 964,
e.mail: marco.montemurro@ensam.eu,
marco.montemurro@u-bordeaux1.fr

*Corresponding author.

Abstract

In this work a multi-scale two-level (MS2L) optimisation strategy for optimising VAT composites is presented. In the framework of the MS2L methodology, the design problem is split and solved into two steps. At the first step the goal is to determine the optimum distribution of the laminate stiffness properties over the structure (macroscopic scale), while the second step aims at retrieving the optimum fibres-path in each layer meeting all the requirements provided by the problem at hand (mesoscopic scale). The MS2L strategy has been improved in order to integrate all types of requirements (mechanical, manufacturability, geometric, etc.) within the first-level problem. The proposed approach relies on: a) the polar formalism for describing the behaviour of the VAT laminate, b) the iso-geometric surfaces for describing the spatial variation of both the laminate stiffness properties (macro-scale) and the layers fibres-path (meso-scale) and c) an hybrid optimisation tool (genetic and gradient-based algorithms) to perform the solution search. The effectiveness of the MS2L strategy is proven through a numerical example on the maximisation of the first buckling factor of a VAT plate subject to both mechanical and manufacturability constraints.

Keywords:

VAT Laminates; Optimisation; Buckling; Genetic Algorithms; B-splines; Composite Materials.

1 Introduction

Anisotropic materials, such as fibres-reinforced composite materials, are extensively used in many industrial fields thanks to their mechanical performances: high stiffness-to-weight and strength-to-weight ratios that lead to a substantial weight saving when compared to metallic alloys. In addition, the recent development of new manufacturing techniques of composite structures, e.g. automated fibre placement (AFP) machines, allows for going beyond the classical design rules, thus leading the designer to find innovative and more efficient solutions than the classical straight fibre configurations. The use of the AFP technology brought to the emergence of a new class of composite materials: the variable angle tow (VAT) composites, [1, 2]. A modern AFP machine allows the fibre (i.e. the tow) to be placed along a curvilinear path within the constitutive lamina thus implying a point-wise variation of the material properties (stiffness, strength, etc.). Of course, this technology enables the designer to take advantage of the directional properties of composites in the most effective way. The interest of using variable stiffness (VS) laminates is considerably increased during the last years: in the meantime some works on the *a posteriori* characterisation of the elastic response of such materials have gained a lot of attention from the scientific community of composites materials, [3, 4]. Although the utilisation of VAT laminates considerably increases the complexity of the design process (mainly due to the large number of design variables involved within the problem), on the other hand it leads the designer to conceive non-conventional solutions characterised either by a considerable weight saving or enhanced mechanical properties when compared to classical solutions, [5, 6, 7, 8]. One of the first works that tried to explore the advantages that can be achieved in terms of mechanical performances (stiffness, buckling behaviour, etc.) by using a VS plate in which each ply is characterised by a curvilinear path of the tow (i.e. a VAT configuration) instead of the conventional straight fibre format is presented in [2]. The authors make use of a sensitivity analysis and a gradient-based search technique to determine the optimal fibre orientation in a given number of regions of the plate. This work proved that a considerable increment of the buckling load of the structure can be obtained when employing a VAT solution for the layered plate.

The complexity of the design process of a VAT laminated structure is mainly due to two intrinsic properties of VAT composites, i.e. the heterogeneity and the anisotropy that intervene at different scales of the problem and that vary point-wise over the structure. Moreover, a further difficulty is due to the fact that such a problem is intrinsically a multi-scale design problem: in the most general case, the designer should take into account, within the same design process, the full set of design variables (geometrical and material) governing the behaviour of the structure at each characteristic scale (micro-meso-macro). Up to now no general rules and methods exist for the optimum design of VAT laminates. Only few works on this topic can be found in literature, and all of them always make use of some simplifying hypotheses and rules to get a solution. An exhaustive review focusing on constant and variable stiffness design of composite laminates is presented in [9, 10]. In [11] the first natural frequency of VS composite panels is maximised by considering on the one hand the lamination parameters and the classical laminate theory (CLT) for the description of the local stiffness properties of the structure and, on the other hand, a generalised reciprocal approximation algorithm for the resolution of the optimisation problem. This approach is limited to the determination of the stiffness properties of an equivalent homogeneous plate, since the lay-up design phase is not at all considered. In [12] the least-weight design problem of VAT laminates submitted to constraints including the strength and the radius of curvature is considered. The design variables are the layers thickness and fibres angles which are represented by bi-cubic Bezier surfaces and cubic Bezier curves, respectively. A sequential quadratic programming method is used to solve the optimisation problem.

A two-level strategy was employed in [13] to design a VAT laminated plate: this work represents the first attempt of applying a multi-scale numerical strategy which aims at determining, at the first level, the optimum distribution of the stiffness properties of the structure (in terms of the lamination parameters of the laminate), while at the second level the optimum path (in each constitutive layer) matching locally the lamination parameters resulting from the first step. However, the major drawback of this work actually was in the determination of the curvilinear fibres-path of each layer: the resulting path was discontinuous because the authors had not foreseen a numerical strategy able to simultaneously meet on the one hand the continuity of the fibres path (between adjacent elements) and on the other hand the optimum distribution of lamination parameters provided by the first step of the procedure. In [14] the two-level approach was abandoned and the authors stated the problem by directly considering the fibres path in each ply as design variables. However, as in [11], this approach always leads to a discontinuous fibres-path and, unlike the strategy proposed in [11], it leads also to the emergence of a new issue: the resulting optimisation problem was highly non-convex since it was formulated directly in the space of the layers orientations (which vary locally over the plate). Accordingly, in [14] the authors conclude that such an issue can be potentially remedied by formulating in a proper way the design problem of VAT laminates in the framework of the two-level strategy and by trying to overcome the issue of the continuity of the fibres-path directly in the first level of the strategy where the design variables are the laminate mechanical properties (e.g. the lamination parameters as in the theoretical framework of [13]).

Another issue often addressed by researches on VAT laminates concerns the tow placement technology which could introduce several differences (i.e. imperfections) between the numerical model of the VAT composite and the real structure tailored with the AFP process, if the design methodology does not take into account the manufacturability requirements. To this purpose in [15] an issue linked to the AFP technology is addressed: the overlap of tow-placed courses that increases the ply thickness (the build-up phenomenon) thus affecting the structural response and the surface quality of the laminate. The work of Blom *et al.* [15] presents a method for designing composite plies with varying fibres angles. The fibre angle distribution per ply is given while, using a streamline analogy, the optimal distributions of fibres courses is determined for minimising the maximum ply thickness or maximising the surface smoothness. An improved research on this topic has been developed in [16] where an algorithm is presented to optimise the fibres path in order to ensure manufacturability. A further work focusing on the development and/or improvement of manufacturing techniques for tailoring VAT laminates in order to minimise the imperfections induced by the fabrication process is presented in [17]. The continuous tow shearing (CTS) technique, utilising the ability to shear dry tows, is proposed as an alternative technique to the well-known AFP process. Later, the work presented in [17] has been improved through the introduction of a computer-aided modelling tool [18] which can create accurate finite element models reflecting the fibre trajectories and thickness variations of VAT composites manufactured using the CTS technique.

To overcome the previous restrictions, recently the authors presented in [19] a first work focused on the generalisation and extension of the multi-scale bi-level (MS2L) procedure for the optimum design of composite structures (initially introduced in [20, 21]) to the case of VAT composites. Such a MS2L procedure has already been employed by the authors and their co-workers in the past for the design and optimisation of several classes of hybrid anisotropic structures [22, 23, 24, 25, 26, 20, 21, 27]. The MS2L design strategy is characterised on the one hand by the refusal of simplifying hypotheses and classical rules usually employed in the framework of the design process of laminates, and on the other hand by a proper and complete mathematical formalisation of the optimum design problem at each characteristic scale (meso-macro). The MS2L strategy relies on the use of the polar formalism (initially introduced by Verchery [28], and later extended to the case of higher-order theories by Montemurro [29, 30, 31]) for the description of the anisotropic behaviour of the composite. The real advantage in using the Verchery's polar method is in the fact that the elastic response of the structure at the macro-scale is described in terms of tensor invariants, the so-called *polar parameters* having a precise physical meaning (which is linked to the elastic symmetries of the material) [32]. On the other hand the MS2L strategy relies on the use of a particular genetic algorithm (GA) able to deal with a special class of huge-size optimisation problems (from hundreds to thousands of design variables) defined over a domain of variable dimension, i.e. optimisation problems involving a "variable number" of design variables [25].

As far as concerns the problem of designing VAT composites in [19] several modifications have been introduced in the theoretical and numerical framework of the MS2L design procedure at both first and second levels. At the first level (laminate macroscopic scale) of the procedure, where the VAT laminate is modelled as an equivalent homogeneous anisotropic plate whose mechanical behaviour is described in terms of polar parameters (which vary locally over the structure) the major modifications concerned: 1) the utilisation of higher-order theories (First-order Shear Deformation Theory (FSDT) framework [29, 30]) for taking into account the influence of the transverse shear stiffness on the overall mechanical response of VAT composites; 2) the utilisation of B-spline surfaces for obtaining a continuous point-wise variation of the laminate polar parameters. Regarding the second-level problem (laminate mesoscopic scale, i.e. the ply level) the main modifications were: 1) the utilisation of B-spline surfaces for obtaining a continuous point-wise variation of the fibres-path within each ply; 2) a proper mathematical formalisation of the manufacturability constraints linked to the AFP process in the framework of the B-spline representation. All of these modifications imply several advantages for the resolution of the related optimisation problems (both at first and second level of the strategy) as detailed in [19]. However, the major drawback of the approach proposed in [19] is in the fact that the manufacturability constraints have been introduced only within the second step of the design procedure. Actually, when using such an approach, there is no warranty that the optimisation algorithm could find an optimum fibres path able to meet on the one hand the optimum distribution of the laminate polar parameters resulting from the first step and on the other hand the manufacturability constraints imposed during the second step.

To overcome such an issue, in the present work the theoretical formulation of the design problem of VAT laminates together with the related MS2L optimisation strategy have been improved: in particular the manufacturability constraints are now integrated within the first-level problem (the structural optimisation) while the second-level problem (the lay-up design) is now formulated as an unconstrained minimisation problem as all the requirements (geometrical, technological, mechanical, etc.) are satisfied since the first step of the MS2L strategy. The paper is organised as follows: the design problem and the MS2L strategy are discussed in Section 2. The mathematical formulation of the first-level problem is detailed in Section 3, while the mathematical statement of the second-level problem (the lay-up design) is presented in Section 4. A concise description of the Finite Element (FE) model of the VAT laminated plate is given in Section 5, while the numerical results of the optimisation procedure are shown in Section 6. Finally, Section 7 ends the paper with some concluding remarks.

2 A new design paradigm for VAT laminates

2.1 Description of the problem

The optimisation strategy presented in this study is applied to a VAT laminated plate composed of a fixed number of plies, hence the total thickness of the plate is fixed *a priori*. The fibres-tow is made of carbon-epoxy pre-preg strips whose elastic properties are listed in Table 1.

Concerning the mechanical behaviour of the VAT plate, further details have to be added in order to clearly define the theoretical framework of this work:

- the geometry of the laminated structure and the applied Boundary Conditions (BCs) are known and fixed;
- the VAT plate is composed of identical plies (i.e. same material and thickness);
- the material behaviour is linear elastic;
- the VAT plate is quasi-homogeneous and fully orthotropic [22, 23, 27, 19] point-wise, i.e. these properties apply locally in each point of the structure;
- at the macro-scale (i.e. the scale of the structure) the elastic response of the VAT plate is described in the theoretical framework of the FSDT and the stiffness matrices of the plate are expressed in terms of the laminate polar parameters [29, 30] which constitute also the design variables of the VAT plate at the macroscopic scale.

As far as concerns the mesoscopic scale of the VAT laminate (i.e. that of the constitutive ply) no simplifying hypotheses are made on the rest of the design parameters of the laminated plate, i.e. the design variables of the stack, namely the layer position and orientation angle (which varies point-wise for each layer).

2.2 Description of the multi-scale two-level optimisation strategy

The main goal of the design strategy is the maximisation of the first buckling load of a VAT plate subject to

- feasibility constraints on the mechanical parameters (i.e. the laminate polar parameters) governing the behaviour of the structure at the macroscopic scale;
- manufacturability constraints on the local radius of the tow (i.e. the local steering) due to the considered AFP technology.

The optimisation procedure is articulated into the following two distinct (but linked) optimisation problems.

1. **First-level problem**. The aim of this phase is the determination of the optimum distribution of the mechanical design variables of the VAT structure in order to minimise the considered objective function and to meet, simultaneously, the full set of optimisation constraints provided by the problem at hand. At this level the VAT composite plate is modelled as an equivalent homogeneous anisotropic continuum whose behaviour is described in terms of laminate polar parameters, which vary point-wise over the structure and constitute the design variables of the first-level problem. Moreover, thanks to a proper formulation of the optimisation problem (detailed in Section 3), at this stage the designer can add further requirements, e.g. manufacturability constraints, strength and damage criteria, etc. by acting directly on the resulting distribution of the laminate polar parameters.

2. **Second-level problem**. The purpose of this design phase is the determination of the optimum lay-up of the laminate composing the structure meeting the optimum distribution of the polar parameters provided by the first level of the strategy. At this stage, the design variables are the layer orientation angles which vary point-wise in each ply (namely the fibres-path).

It is noteworthy that the integration of the manufacturability constraints within the first-level problem implies some important consequences on the formulation as well as on the resolution technique of the second-level problem that will be detailed in Section 4.

3 Mathematical formulation of the first-level problem

As discussed in [19], in order to apply the MS2L numerical optimisation strategy [23, 27] to the case of VAT composites some major modifications have been introduced. Regarding the first-level problem these modifications focus on:

- the utilisation of higher-order theories (in this case the FSDT) for taking into account the influence of the transverse shear stiffness on the overall mechanical response of the VAT laminate;
- the utilisation of B-spline surfaces for expressing the variation of the laminate polar parameters over the structure.

The first point represents a very important step forward in the MS2L strategy when applied to every kind of composite structure (classical or VAT) as it allows to properly design thin as well as moderately thick plates.

The second modification leads to important consequences, too. Such consequences constitute just as many advantages for the resolution of the related optimisation problem. Firstly, the utilisation of iso-geometric surfaces leads to a considerable reduction in the number of mechanical design variables (at the macro-scale), i.e. the polar parameters defined in each point of the *control net* of the B-spline surface. Secondly, thanks to the *strong convex hull property* of the B-spline blending functions the optimisation constraints of the problem, related to the specifications of the considered application, can be imposed only on the control points of the net: if they are satisfied on such points they are automatically met over the whole domain.

However, in the present work, in order to integrate the manufacturability constraints within the mathematical formulation of the first-level problem further modifications have been introduced:

- only the variation of one polar parameter (namely the polar angle, as discussed in the next subsection) is described in terms of iso-geometric surface over the plate, while the others are kept constant;
- thanks to the previous assumption, the technological constraint on the minimum admissible radius of curvature of the tow can be directly imposed on the B-spline surface describing the variation of the polar angle.

These last aspects are of paramount importance: due to the functional relationship existing between the polar angle and the plies orientation angles [29, 30], whether the manufacturability constraint is satisfied by the optimum distribution of the polar angle over the plate it will be automatically met also by the B-spline surfaces describing the variation of the fibres path in each layer as discussed in Section 4.

As previously stated the goal of the first level of the strategy is the maximisation of the buckling load of the VAT laminate by simultaneously satisfying the feasibility and manufacturability constraints on the distribution of the laminate polar parameters over the plate. All of these aspects are detailed in the following subsection.

3.1 Mechanical design variables

In the framework of the FSDT theory [33] the constitutive law of the laminated plate (expressed within the global frame of the laminate $R = \{0; x, y, z\}$) can be stated as:

$$\left\{ \begin{array}{c} \{\mathrm{N}\} \\ \{\mathrm{M}\} \end{array} \right\} = \begin{bmatrix} [\mathrm{A}] & [\mathrm{B}] \\ [\mathrm{B}] & [\mathrm{D}] \end{bmatrix} \left\{ \begin{array}{c} \{\varepsilon_0\} \\ \{\chi_0\} \end{array} \right\} , \tag{1}$$

$$\{\mathrm{F}\} = [\mathrm{H}] \{\gamma_0\} \ , \tag{2}$$

where [A], [B] and [D] are the membrane, membrane/bending coupling and bending stiffness matrices of the laminate, while [H] is the out-of-plane shear stiffness matrix. {N}, {M} and {F} are the vectors of membrane forces, bending moments and shear forces per unit length, respectively, whilst $\{\varepsilon_0\}$, $\{\chi_0\}$ and $\{\gamma_0\}$ are the vectors of in-plane strains, curvatures and out-of-plane shear strains of the laminate middle plane, respectively, [33].

In order to analyse the elastic response of the multilayer plate the best practice consists in introducing the laminate homogenised stiffness matrices defined as:

$$\begin{aligned}
&[\mathrm{A}^*] = \frac{1}{h}[\mathrm{A}] \qquad , \\
&[\mathrm{B}^*] = \frac{2}{h^2}[\mathrm{B}] \qquad , \\
&[\mathrm{D}^*] = \frac{12}{h^3}[\mathrm{D}] \qquad , \\
&[\mathrm{H}^*] = \begin{cases} \dfrac{1}{h}[\mathrm{H}] & \text{(basic)} \quad , \\ \dfrac{12}{5h}[\mathrm{H}] & \text{(modified)} \quad . \end{cases}
\end{aligned} \tag{3}$$

where h is the total thickness of the laminated plate.

As discussed in [29, 30], in the framework of the polar formalism it is possible to express the Cartesian components of these matrices in terms of their elastic invariants: it can be proven that, also in the FSDT theoretical framework, in the case of a fully orthotropic, quasi-homogeneous laminate the overall number of independent mechanical design variables describing its mechanical response reduces to only three, i.e. the anisotropic polar parameters $R_{0K}^{A^*}$ and $R_1^{A^*}$ and the polar angle $\Phi_1^{A^*}$ (this last representing the orientation of the main orthotropy axis) of the homogenised membrane stiffness matrix $[\mathrm{A}^*]$. For more details on the polar formalism and its application in the context of the FSDT the reader is addressed to [29, 30, 32].

For a VAT composite, in the most general case, all of the three independent polar parameters can vary point-wise over the structure [19]. However, the aim of this work is to improve the MS2L procedure in order to integrate the manufacturability constraint on the local steering (i.e. the local radius of curvature of the tow) since the first step of the strategy. To achieve this goal a simplification must be imposed: only the polar angle $\Phi_1^{A^*}$ can vary over the structure (and such a variation is expressed by means of a B-spline surface) while $R_{0K}^{A^*}$ and $R_1^{A^*}$ are kept constant. In particular, in the mathematical framework of the B-spline surfaces the variation of the laminate polar angle $\Phi_1^{A^*}$ can be expressed as:

$$\Phi_1^{A^*}(\xi,\gamma) = \sum_{i=0}^{n_p}\sum_{j=0}^{m_p} N_{i,p}(\xi)\, N_{j,q}(\gamma)\, \Phi_1^{A^*(i,j)}. \tag{4}$$

Eq. (4) fully describes a B-spline surface of degrees p and q along the parametric coordinates ξ and γ, respectively, as depicted in Fig. 1.

The dimensionless coordinates ξ and γ can be arbitrarily defined: a natural choice consists of linking them to the Cartesian coordinates of the laminated plate,

$$\xi = \frac{x}{a}\ , \gamma = \frac{y}{b}\ , \tag{5}$$

where a and b are the lengths of the plate edges along x and y axes, respectively. In Eq.(4) $\Phi_1^{A^*(i,j)}$ $(i = 0, \cdots, n_p,\ j = 0, \cdots, m_p)$ is the value of the laminate polar angle at the generic control point (the set of $(n_p+1) \times (m_p+1)$ control points forms the so-called *control network*), while $N_{i,p}(\xi)$ and $N_{j,q}(\gamma)$ are the p^{th}-degree and q^{th}-degree B-spline basis functions (along ξ and γ directions, respectively) defined on the non-periodic, non-uniform knot vectors:

$$\begin{aligned}
\boldsymbol{\Xi} &= \Big\{\underbrace{0,\cdots,0}_{p+1}, \Xi_{p+1}, \cdots, \Xi_{r-p-1}, \underbrace{1,\cdots,1}_{p+1}\Big\}\ ,\\
\boldsymbol{\Gamma} &= \Big\{\underbrace{0,\cdots,0}_{q+1}, \Gamma_{q+1}, \cdots, \Gamma_{s-q-1}, \underbrace{1,\cdots,1}_{q+1}\Big\}\ .
\end{aligned} \tag{6}$$

It is noteworthy that the dimensions of the knot-vectors $\boldsymbol{\Xi}$ and $\boldsymbol{\Gamma}$ are $r+1$ and $s+1$, respectively, with:

$$\begin{aligned}
r &= n_p + p + 1\ ,\\
s &= m_p + q + 1\ .
\end{aligned} \tag{7}$$

For a deeper insight in the matter the reader is addressed to [34].

This new formulation of the mechanical design variables of the first-level problem allows the designer to impose the manufacturability constraints directly on the spatial distribution of the polar angle $\Phi_1^{A^*}$: if this requirement is met at this stage of the strategy it will be automatically met by the optimum lay-up resulting from the second-level problem without imposing further constraints, as detailed in Section 4. Furthermore, this formulation is characterised by the following advantages:

- the use of an iso-geometric surface for describing the variation of $\Phi_1^{A^*}$ over the structure implies that the three independent polar parameters have no discontinuity over the plate ($R_{0K}^{A^*}$ and $R_1^{A^*}$ being constant);

- thanks to the B-spline representation the laminate polar angle must be determined solely on each point of the *control net*, implying in this way a significant reduction in the number of design variables involved within the first-level problem.

Therefore, the optimisation variables of the problem can be grouped into the vector:

$$\mathbf{x} = \left\{ \Phi_1^{A^*(0,0)}, \cdots, \Phi_1^{A^*(n_p,m_p)}, R_{0K}^{A^*}, R_1^{A^*} \right\} \ . \tag{8}$$

The total number of design variables is hence equal to $2 + (n_p + 1) \times (m_p + 1)$.

Thanks to the utilisation of the B-spline surface for representing the spatial variation of $\Phi_1^{A^*}$, the technological constraint on the minimum admissible radius of curvature of the tow can be stated in a straightforward way:

$$g_1(\mathbf{x}) = r_{adm} - r_{min} \leq 0 \ , \tag{9}$$

where r_{adm} is the minimum admissible radius of curvature of the tow whose value depends upon the AFP process, while r_{min} is the local least radius of curvature of the B-spline surface describing the variation of $\Phi_1^{A^*}$. r_{min} is defined as:

$$\begin{aligned} &r_{min} = \min_{(x,y)} r(x,y) \ , \\ &r(x,y) = \left(\mathbf{t} \cdot \nabla\Phi_1^{A^*}\right)^{-1} \ , \quad \begin{aligned} x &\in [0, \ a] \ , \\ y &\in [0, \ b] \ . \end{aligned} \end{aligned} \tag{10}$$

In Eq. (10) $\mathbf{t}$ is the local tangent vector of the angular field ${\Phi_1}^{A^*}(x,y)$, while $\nabla\Phi_1^{A^*}$ is the gradient of the orthotropy orientation with respect to coordinates (x,y), namely

$$\begin{aligned} \mathbf{t} &= \left\{\cos\Phi_1^{A^*} \ , \sin\Phi_1^{A^*}\right\} \ , \\ \nabla\Phi_1^{A^*} &= \left\{ \frac{1}{a}\frac{\partial\Phi_1^{A^*}}{\partial\xi} \ , \frac{1}{b}\frac{\partial\Phi_1^{A^*}}{\partial\gamma} \right\} \ . \end{aligned} \tag{11}$$

In addition, in the formulation of the optimisation problem for the first level of the strategy, the geometric and feasibility constraints on the polar parameters (which arise from the combination of the layers orientations and positions within the stack) must also be considered. These constraints ensure that the optimum values of the polar parameters resulting from the first step correspond to a feasible laminate that will be designed during the second step of the optimisation strategy, see [35]. Since the laminate is quasi-homogeneous, such constraints can be written only for matrix [A*] as follows:

$$\begin{cases} -R_0 \leq R_{0K}^{A^*} \leq R_0 \ , \\ 0 \leq R_1^{A^*} \leq R_1 \ , \\ 2\left(\dfrac{R_1^{A^*}}{R_1}\right)^2 - 1 - \dfrac{R_{0K}^{A^*}}{R_0} \leq 0 \ . \end{cases} \tag{12}$$

First and second constraints of Eq. (12) can be taken into account as admissible intervals for the relevant optimisation variables, i.e. on $R_{0K}^{A^*}$ and $R_1^{A^*}$. Hence, the resulting feasibility constraint on the laminate polar parameters is:

$$g_2(\mathbf{x}) = 2\left(\frac{R_1^{A^*}}{R_1}\right)^2 - 1 - \frac{R_{0K}^{A^*}}{R_0} \leq 0 \ . \tag{13}$$

For a wide discussion upon the laminate feasibility and geometrical bounds as well as on the importance of the quasi-homogeneity assumption the reader is addressed to [35].

3.2 Mathematical statement of the problem

The first-level problem focuses on the definition of the optimal distribution of the laminate polar parameters. In this background, the solution of the structural optimisation problem is searched for an orthotropic and quasi-homogeneous (point-wise) plate subject to given BCs.

Therefore the optimisation problem can be formulated as follows:

$$\begin{aligned} &\min_{\mathbf{x}} \quad -\lambda\left(\mathbf{x}\right) \\ &\text{subject to:} \\ &\ g_i(\mathbf{x}) \leq 0 \ , \ \ (i = 1, 2) \end{aligned} \tag{14}$$

where λ is the first buckling factor of the laminated structure.

3.3 Numerical strategy

Problem (14) is a non-linear, non-convex problem in terms of the mechanical design variables. Its non-linearity and non-convexity is due to the nature of the objective function, the first buckling factor, that is a non-convex function in terms of the orthotropy orientation. In addition, the complexity of such a problem is also due to the feasibility and manufacturability constraints imposed on the polar parameters of the plate, see Eqs. (9) and (13). We recall that the overall number of design variables and optimisation constraints for problem (14) is $2 + (n_p + 1) \times (m_p + 1)$ and two, respectively.

For the resolution of problem (14) a hybrid optimisation tool, composed of the GA BIANCA [25] interfaced with the MATLAB *fmincon* algorithm [36], coupled with a FE model of the plate (used for numerical calculation of the first buckling load) has been developed, see Fig. 2.

The GA BIANCA was already successfully applied to solve different kinds of real-world engineering problems, e.g. [23, 27]. As shown in Fig. 2, the optimisation procedure for the first-level problem is split in two phases. During the first phase the GA BIANCA is interfaced with the FE model of the VAT plate: for each individual at each generation, a FE-based buckling analysis is carried out for the evaluation of the first buckling load of the structure. The FE model makes use of the mechanical design variables, given by BIANCA and elaborated by an ANSYS Parametric Design Language (APDL) macro which generates the B-spline surface representing the distribution of the polar angle $\Phi_1^{A^*}$ over the VAT plate, in order to calculate the first buckling load of the structure together with the minimum radius of curvature of the angular field. At the end of the FE analysis, the GA elaborates the results provided by the FE model (in terms of objective and constraint functions) in order to execute the genetic operations. These operations are repeated until the GA meets the user-defined convergence criterion.

The generic individual of the GA represents a potential solution for the problem at hand. The genotype of the individual for problem (14) is illustrated in Fig. 3 and it is characterised on the one hand by a modular part composed of $(n_p + 1) \times (m_p + 1)$ chromosomes with only one gene coding the value of the polar angle $\Phi_1^{A^*(i,j)}$ while on the other hand by a fixed chromosome with only two genes each one coding the remaining polar parameters, i.e. $R_{0K}^{A^*}$ and $R_1^{A^*}$. Due to the strong non-convex nature of problem (14), the aim of the genetic calculation is to provide a potential sub-optimal point in the design space which constitutes the initial guess for the subsequent phase, i.e. the local optimisation, where the *fmincon* gradient-based algorithm is interfaced with the same FE model of the VAT plate.

4 Mathematical formulation of the second-level problem

The second-level problem concerns the lay-up design of the VAT laminated plate. The goal of this problem is the determination of at least one stacking sequence satisfying the optimum spatial distribution of the polar parameters over the structure resulting from the first level of the strategy and having the elastic symmetries imposed to the laminate within the formulation of the first-level problem, i.e. quasi-homogeneity and orthotropy.

In the case of a VAT solution the fibres-path varies point-wise in every ply composing the laminate. Hence a proper description of the fibres-path is necessary to formulate and solve the second-level problem of the MS2L strategy. To this purpose, the point-wise variation of the fibres orientation (in each ply) is described through the use of a B-spline surface. As explained in [19] the use of B-spline surfaces allows, as in the case of the first-level problem, to reduce the total number of design variables.

Nevertheless, unlike the approach proposed in [19], the improved formulation of the first-level problem along with the integration of the manufacturability constraints described in Section 3 lead to some major modifications (and simplifications) also for the second-level problem. In particular, as in [19] the fibres-path in the generic ply is represented through a B-spline surface as:

$$\delta_k(\xi,\gamma) = \sum_{i=0}^{n_p}\sum_{j=0}^{m_p} N_{i,p}(\xi)\, N_{j,q}(\gamma)\, {\delta_k}^{(i,j)} \quad \text{with} \quad k = 1, \cdots, n\ , \tag{15}$$

where ${\delta_k}^{(i,j)}$ is the orientation angle at the generic control point for the k-th layer. Moreover, this B-spline surface is characterised by the same parameters (with the exception of the value of the orientation in each control point) as those utilised for the definition of the B-spline surface of the polar angle $\Phi_1^{A^*}(\xi, \gamma)$, see Eqs. (4)-(7).

As a consequence of both the new formalisation of the first-level problem and the assumptions made on the spatial distribution of the polar parameters of the laminate, the value of the fibre orientation angle in each control point (for each layer) can be calculated as follows:

$$
{\delta_k}^{(i,j)} = \Phi_1^{A^*(i,j)} + \delta_k(\xi_0, \gamma_0) - {\Phi_1}^{A^*}(\xi_0, \gamma_0) \ , \tag{16}
$$

where $\delta_k(\xi_0, \gamma_0)$ and ${\Phi_1}^{A^*}(\xi_0, \gamma_0)$ are the fibres orientation angle for the k-th layer and the local orthotropy orientation of the laminate, respectively, calculated at the arbitrary point (ξ_0, γ_0). As it clearly appears from Eq. (16) the only unknowns are the layer orientation angles $\delta_k(\xi_0, \gamma_0)$. Therefore, in this background (and unlike the approach proposed in [19]) the design variables of the second-level problem are not the layers orientation angles in each point of the control net, rather the value of the orientation angle at the arbitrary point (ξ_0, γ_0) for each ply, namely $\delta_k(\xi_0, \gamma_0)$. This fact implies some consequences of paramount importance which constitutes as many advantages in the formalisation and resolution of the second-level problem.

Firstly, when compared to the approach presented in [19] the number of design variables of the second-level problem is drastically reduced and passes from $n \times (n_p + 1) \times (m_p + 1)$ to only n, i.e. the plies orientation angles defined for the arbitrary pair (ξ_0, γ_0).

Secondly, the second-level problem can now be formulated as an unconstrained minimisation problem (because the manufacturability constraints are integrated into the first stage of the MS2L strategy) and solved solely in one (arbitrary) point of the VAT laminated plate:

$$
\min_{\delta_k(\xi_0, \gamma_0)} \quad I(\delta_k(\xi_0, \gamma_0)) \quad k = 1, \cdots, n \ . \tag{17}
$$

In Eq. (17) $I(\delta_k(\xi_0, \gamma_0))$ is the overall objective function which is defined as:

$$
I(\delta_k(\xi_0, \gamma_0)) = \sum_{i=1}^{6} f_i(\delta_k(\xi_0, \gamma_0)) \ . \tag{18}
$$

where $f_i(\delta_k(\xi_0, \gamma_0))$ are quadratic functions in the space of polar parameters, each one representing a requirement to be satisfied. For the problem at hand the partial objective functions write:

$$
\begin{aligned}
f_1(\delta_k(\xi_0,\gamma_0)) &= \left[\frac{\Phi_0^{A^*}(\delta_k(\xi_0,\gamma_0)) - \Phi_1^{A^*}(\delta_k(\xi_0,\gamma_0))}{\pi/4} - K^{A^*(opt)}\right]^2 ,\\
f_2(\delta_k(\xi_0,\gamma_0)) &= \left[\frac{R_0^{A^*}(\delta_k(\xi_0,\gamma_0)) - R_0^{A^*(opt)}}{R_0}\right]^2 ,\\
f_3(\delta_k(\xi_0,\gamma_0)) &= \left[\frac{R_1^{A^*}(\delta_k(\xi_0,\gamma_0)) - R_1^{A^*(opt)}}{R_1}\right]^2 ,\\
f_4(\delta_k(\xi_0,\gamma_0)) &= \left[\frac{\Phi_1^{A^*}(\delta_k(\xi_0,\gamma_0)) - \Phi_1^{A^*(opt)}(\xi_0,\gamma_0)}{\pi/4}\right]^2 ,\\
f_5(\delta_k(\xi_0,\gamma_0)) &= \left[\frac{||\,[\mathrm{C}]\,(\delta_k(\xi_0,\gamma_0))||}{||\,[\mathrm{Q}]\,||}\right]^2 ,\\
f_6(\delta_k(\xi_0,\gamma_0)) &= \left[\frac{||\,[\mathrm{B}^*]\,(\delta_k(\xi_0,\gamma_0))||}{||\,[\mathrm{Q}]\,||}\right]^2 ,
\end{aligned}
\tag{19}
$$

where

$$
K^{A^*(opt)} = \begin{cases} 1 & \text{if} \qquad R_{0K}^{A^*(opt)} < 0 \ , \\ 0 & \text{otherwise} \ . \end{cases}
\tag{20}
$$

In Eq. (19) $f_1(\delta_k(\xi_0,\gamma_0))$ represents the elastic requirement on the orthotropy of the laminate having the prescribed shape, $f_2(\delta_k(\xi_0,\gamma_0))$, $f_3(\delta_k(\xi_0,\gamma_0))$ and $f_4(\delta_k(\xi_0,\gamma_0))$ are the requirements related to the prescribed values of the optimal polar parameters resulting from the first-level problem, while $f_5(\delta_k(\xi_0,\gamma_0))$ and $f_6(\delta_k(\xi_0,\gamma_0))$ are linked to the quasi-homogeneity condition. For more details on the meaning of the partial objective functions, on the elastic symmetries of the laminate in the framework of the FSDT and on the symbols appearing in Eq. (19), the reader is addressed to [29, 30]. $I(\delta_k(\xi_0,\gamma_0))$ is a positive semi-definite convex function in the space of laminate polar parameters, since it is defined as a sum of convex functions, see Eqs. (18)-(19). Nevertheless, such a function is highly non-convex in the space of plies orientations because the laminate polar parameters depend upon circular functions of the layers orientation angles, see [29, 30]. Moreover, one of the advantages of such a formulation consists in the fact that the absolute minima of $I(\delta_k(\xi_0,\gamma_0))$ are known a priori since they are the zeroes of this function. For more details about the nature of the second-level problem see [25, 26, 21].

Concerning the numerical strategy for solving problem (17) the GA BIANCA has been employed to find a solution also for the second-level problem. In the most general case, the genotype of the individual is composed of n chromosomes (one for each ply), each one characterised by a single gene coding the layer orientation angle.

5 Finite element model of the VAT laminate

In order to determine the current value of the objective function (the first buckling factor) and that of the optimisation constraints of problem (14) a classical eigenvalue buckling analysis must be achieved for the VAT composite. The need to analyse, within the same calculation, different configurations of the VAT plate requires the creation of an *ad-hoc* input file for the FE model that has to be interfaced with the hybrid (GA + gradient-based algorithms) optimisation tool.

The FE model of the VAT laminated plate (see Fig. 4) employed during the first step of the MS2L strategy, is built within the ANSYS environment and is made of SHELL281 elements based on the Reissner-Mindlin kinematic model, having 8 nodes and six Degrees Of Freedom (DOFs) per node. The mesh size is chosen after preliminary mesh sensitivity analyses on the convergence of the value of the first buckling load for a given set of BCs. It was observed that a mesh having 2482 DOFs is sufficient to properly evaluate the first buckling load of the structure.

It is noteworthy that the B-Spline mathematical formalism has been implemented by the authors into the ANSYS environment by using the APDL [37] for creating a set of appropriate macros that were integrated within the FE model of the VAT plate. At this stage, the plate is modelled as an equivalent homogeneous anisotropic plate whose stiffness matrices ([A*], [B*], [D*] and [H*]) vary point-wise, i.e. for each element discretising the real structure. In particular, in order to properly define, for every element of the VAT plate, the correct value of its stiffness properties the following strategy has been employed:

1. for a given set of the laminate polar parameters defined in each control point (i.e. the design variables passed from the optimisation tool to the FE model of the VAT plate), build the corresponding B-spline surfaces;

2. discretise the plate into N_e elements;

3. fix the element index i: for the i-th element retrieve the Cartesian coordinates of its centroid, i.e. (x_e^i, y_e^i) and calculate the corresponding dimensionless coordinates (ξ_e^i, γ_e^i) according to Eq. (5);

4. calculate the laminate polar parameters (and hence the Cartesian components of the stiffness matrices of the laminate) for (ξ_e^i, γ_e^i) and assign the material properties to the element i;

5. repeat points 3 and 4 for each element of the plate.

Finally, the linear buckling analysis is performed using the BCs depicted in Fig. 4 and listed in Table 2.

6 Studied cases and results

In this section a meaningful numerical example is considered in order to prove the effectiveness of the MS2L strategy for the optimum design of VAT laminates. As depicted in

Fig. 4, a bi-axial compressive load per unit length is applied on the plate edges with a ratio $N_y/N_x = 0.5$. The plate has a square geometry with side length $a = b = 254$ mm and is made of $n = 24$ plies whose material properties are those listed in Table 1. Concerning the first-level problem, the parameters defining the B-spline surface which describe the spatial distribution of the polar angle over the VAT plate are set as: $n_p = m_p = 4$ (hence five control points along each direction), $p = q = 2$ (degrees of the blending functions along each direction). Moreover, the B-spline is defined over the following uniform knot-vectors:

$$\begin{aligned}
&\boldsymbol{\Xi} = \left\{0, 0, 0, \tfrac{1}{3}, \tfrac{2}{3}, 1, 1, 1\right\}, \\
&\boldsymbol{\Gamma} = \left\{0, 0, 0, \tfrac{1}{3}, \tfrac{2}{3}, 1, 1, 1\right\}.
\end{aligned} \tag{21}$$

Accordingly, for the first-level problem the overall number of design variables and optimisation constraints is 27 and two, respectively. The mechanical design variables together with their nature and bounds for the first-level problem are listed in Table 3. In addition, the reference value for the minimum admissible radius of curvature of the tow, i.e. r_{adm} is set equal to 80 mm.

Concerning the second-level problem, the parameters defining the B-spline surface which describes the point-wise variation of the fibre orientation angle (for each ply) are the same as those employed during the first step of the strategy. However, in order to further simplify the problem of retrieving an optimum stack, the search space for problem (17) has been restricted to a particular class of quasi-homogeneous laminates: the *quasi-trivial* (QT) stacking sequences which constitute exact solutions with respect to the requirements of quasi-homogeneity, i.e. functions $f_5(\delta_k(\xi_0, \gamma_0))$ and $f_6(\delta_k(\xi_0, \gamma_0))$ in Eq. (19). QT solutions can be found for laminates with identical plies (same material and thickness) by acting only on the position of the layers within the stack. Indeed, the potential of QT stacks is in the fact that they constitute exact solutions (in terms of quasi-homogeneity condition) regardless to the value of the orientation angle assigned to each layer: in this way the orientations represent free parameters which can be optimised to fulfil further elastic requirements. The procedure for searching QT stacks is (conceptually) quite simple: it suffices to fix the number of layers n and the number of *saturated groups* n_g (i.e. the number of possible different orientation angles within the stack) and look for all the permutations of the position of each group meeting the quasi-homogeneity condition. More details on this topic can be found in [38]. Nevertheless, as discussed in [38], the problem of determining QT stacks gives rise to a huge number of solutions: the number of QT stacks rapidly increases along with n. To this purpose a database of QT stacks has been built for different combinations of n and n_g.

For the problem at hand, and for each considered case, the number of saturated groups n_g has been fixed *a priori*. Let be n_{sol} the number of QT stacks for a particular combination of n and n_g. Each solution collected within the database is uniquely identified by an ID_{sol} (i.e. an integer) which varies in the range $[1, n_{sol}]$. Therefore the ID_{sol} represents a further design variable along with the n_g orientation angles. As stated previously, the solution search is performed through the GA BIANCA; in the case of QT stacks the structure of the individual's genotype is simple because it is composed of a single chromosome with $n_g + 1$ genes: the first one codes the variable ID_{sol} whilst the remaining genes code the orientation angles associated to every group which are continuous variables in the range [-90°, 90°].

Regarding the setting of the genetic parameters for the GA BIANCA utilised for both first and second-level problems they are listed in Table 4. Moreover, concerning the constraint-handling technique for the first-level problem the Automatic Dynamic Penalization (ADP) method has been employed, see [39]. For more details on the numerical techniques developed within the new version of BIANCA and the meaning of the values of the different parameters tuning the GA the reader is addressed to [25, 21].

As far as concerns the *fmincon* optimisation tool employed for the local solution search at the end of the first step, the numerical algorithm chosen to carry out the calculations is the *active-set* method with non-linear constraints. For more details on the gradient-based approaches implemented into MATLAB, the reader is addressed to [36].

Before starting the multi-scale optimisation process a reference structure must be defined in order to establish a reference value for the first buckling factor of the plate. The reference structure is still a square plate of side $a = b = 254$ mm composed of 24 unidirectional fibre-reinforced laminae whose material properties are those listed in Table 1. The stacking sequence of the reference solution is $[0/-45/0/45/90/45/0/-45/90/45/90/-45]_s$. The choice of the reference solution has been oriented towards a symmetric quasi-isotropic stack, of common use in real-world engineering applications, which constitutes a "good" compromise between weight and stiffness requirements (in terms of buckling load): such a configuration is characterised by a buckling factor $\lambda_{ref} = 81.525$ when $N_x = 1$ N/mm and $N_y = 0.5$ N/mm.

6.1 Case 1: design without manufacturability constraints

Problem (14) has been firstly solved to design a VAT plate which is not subject to manufacturability constraints. In this case the only optimisation constraint is that on the feasibility of the polar parameters ${R_{0K}}^{A^*}$ and ${R_1}^{A^*}$, see Eq. (13). Concerning the first-level problem, the optimum distribution of the laminate polar angle ${\Phi_1}^{A^*}$ over the VAT plate is illustrated in Fig. 5, while the optimum value of the polar parameters ${R_{0K}}^{A^*}$ and ${R_1}^{A^*}$ as well as that of ${\Phi_1}^{A^*}$ for each control point are listed in Tables 5 and 6, respectively.

Regarding the solution of the second-level problem, the number of saturated groups n_g is set equal to three. In the case of a laminate composed of 24 plies and three saturated groups the overall number of QT stacks is $n_{sol} = 26$. Assigning the scalars zero, one and two to the first, second and third saturated group, respectively, the optimal stacking sequence provided by the GA is:

$$[0\ 1\ 0\ 1\ 2\ 0\ 2\ 0\ 2\ 2\ 0\ 0\ 0\ 0\ 1\ 1\ 0\ 1\ 0\ 1\ 2\ 0\ 2\ 0]\ . \tag{22}$$

This means that within the optimum stack layers

- 1, 3, 6, 8, 11-14, 17, 19, 22 and 24 belong to the saturated group "0", i.e. they share the same orientation $\delta_0\left(\xi, \gamma\right)$;
- 2, 4, 15, 16, 18 and 20 belong to the saturated group "1" characterised by the local orientation angle $\delta_1\left(\xi, \gamma\right)$;
- 5, 7, 9, 10, 21 and 23 belong to the saturated group "2" sharing the orientation angle $\delta_2\left(\xi, \gamma\right)$.

Since the orientation angle for every saturated group is described by means of a B-spline surface, it suffices to list the value of the orientation in each point of the control net to uniquely define the B-spline surface. To this purpose the optimum values of the orientation angle in each point of the control net for every saturated group are reported in Tables 8-10, whilst an illustration of the optimum fibres-path (for each group) is depicted in Fig. 6.

It is noteworthy that the optimal solution found at the end of the MS2L design procedure is characterised by a buckling factor of 145.74 which is about 78% higher than the reference counterpart and, in the meantime, satisfies the feasibility constraint on the polar parameters.

6.2 Case 2: design including manufacturability constraints

In this section the problem of the optimum design of a VAT laminated plate is solved in the most general case, i.e. by taking into account also the manufacturability constraint on the minimum radius of curvature of the tow imposed by the AFP fabrication process, see Eq. (9). Concerning the first-level problem, the optimum value of the polar parameters ${R_{0K}}^{A^*}$ and ${R_1}^{A^*}$ as well as that of ${\Phi_0}^{A^*}$ for each control point are reported in Tables 5 and 7, respectively, whilst the optimum distribution of the laminate polar angle ${\Phi_0}^{A^*}$ over the VAT plate is illustrated in Fig. 7.

As shown in Table 5, for this second case a particular solution has been obtained: the optimum value of the polar parameter ${R_1}^{A^*}$ is equal to zero in each point of the VAT composite plate which means that locally the structure is characterised by the square elastic symmetry, see [31]. In this case, the main direction of orthotropy is represented (point-wise) by the spatial distribution of the polar angle ${\Phi_0}^{A^*}$. The relationship between the two polar angles, which represents a tensor invariant too, is:

$${\Phi_0}^{A^*} - {\Phi_1}^{A^*} = K^{A^*}\frac{\pi}{4}\ , \tag{23}$$

which applies for every point of the B-spline surface, thus for the points of the control net too. Moreover, in this case $K^{A^*} = 1$ because ${R_{0K}}^{A^*} < 0$, see Table 5.

As far as concerns the solution of the second-level problem, a number of saturated groups $n_g = 4$ has been chosen. In the case of a laminate composed of 24 plies and four saturated groups only one QT stack exists having the form:

$$[0\ 1\ 2\ 3\ 2\ 3\ 1\ 3\ 0\ 2\ 0\ 1\ 0\ 1\ 3\ 1\ 2\ 0\ 2\ 3\ 2\ 3\ 0\ 1]\ , \tag{24}$$

where an integer between zero and three has been assigned to each saturated group. However, in performing the solution search for problem (17), the GA provided an optimum stack with only two saturated groups having the form:

$$[0\ 0\ 2\ 2\ 2\ 2\ 0\ 2\ 0\ 2\ 0\ 0\ 0\ 0\ 2\ 0\ 2\ 0\ 2\ 2\ 2\ 2\ 0\ 0]\ , \tag{25}$$

which means that groups 0 and 1 are identical as well as groups 2 and 3. The optimum values of the orientation angles in each point of the control net for every saturated group are reported in Tables 11 and 12, whilst an illustration of the optimum fibres-path (for each group) is depicted in Fig. 8.

It is noteworthy that the optimal solution found at the end of the MS2L design procedure is characterised by a buckling factor of 136.09 which is about 67% higher than the reference counterpart and, in the meantime, satisfies both the feasibility constraint on the polar parameters and the manufacturability constraint on the minimum (local) radius of curvature of the tow.

6.3 General discussion of results

From a careful analysis of the optimum configuration of the VAT laminated plate provided by the MS2L procedure, it is possible to deduce the following facts.

- The point-wise variation of the laminate polar angles resulting from the first step of the strategy is totally asymmetric. Symmetric solutions are, of course, possible: it is sufficient to impose the symmetry condition directly on the values of the polar angles at the points of the control network of the B-spline surfaces. However, in order to state and solve the optimisation problem in the most general case, such a condition has not been imposed in this study.

- When looking at the optimum spatial distribution of the laminate polar parameters (Tables 5-7), one can notice that the laminate can be characterised either by an ordinary orthotropy shape with $K^{A^*} = 0$ (case 1) as well as by a square symmetry with $R_1^{A^*} = 0$ (case 2). Indeed, in the first case (where the manufacturability constraint is not considered) the spatial distribution of ${\Phi_1}^{A^*}$ over the plate is characterised by a pronounced value of the gradient, hence by small values of the local radius of curvature which "stiffen" the structure by increasing the buckling factor. Conversely, when looking at the solution of case 2 (where the requirement on the local steering is taken into account) the variation of ${\Phi_0}^{A^*}$ is smoother than that of the previous case in order to comply with the manufacturability constraint. Moreover the solution of case 2 is located on the boundary of the elastic domain of the laminate polar parameters, see Table 3. Accordingly, when searching for an optimum stack solution of problem (17) the GA found a point-wise QT symmetric cross-ply stack (indeed the angular difference between the two saturated groups is equal to 90° for each point of the plate, see Tables 11 and 12) whose main axis of orthotropy (i.e. ${\Phi_0}^{A^*}$) varies locally to maximise the buckling factor and to meet, at the same time, the technological constraint.

- Unlike the vast majority of works reported in literature [40], the optimum fibres-path for each ply is very general. In the framework of the proposed approach, the point-wise variation of the fibres-path in every lamina does not follow simple linear or parabolic variations (with respect to laminate global frame), rather it is described by a general B-spline surface, see Eq. (15). This fact, together with the very general formulation of the design problem of VAT laminates, allows the designer to find an optimum stack meeting all the requirements (i.e. elastic and manufacturability constraints) which are integrated directly in the first step of the strategy (i.e. at the macroscopic scale), see Eq. (14), without the need of a further post-processing treatment to simplify the trajectory of the tows in order to comply with the constraints imposed by the AFP process.

- Finally, the optimum fibres-path (for each layer) found at the end of the second step of the MS2L procedure does not need of a further step for the reconstruction of the CAD model because the variation of the fibres-path is described by a B-spline surface which is fully compatible with several standard file formats (IGES, STL and STEP), allowing in this way a rapid exchange of information among the CAD tool and the software of the AFP process.

7 Conclusions

In this work an improved version of the multi-scale two-level design/optimisation methodology of VAT composite structures (initially presented in [19]) has been introduced. This design paradigm essentially relies on the utilisation of a MS2L optimisation procedure characterised by several features that make it an original, effective and general method for the multi-scale design of VAT structures. In the present work this strategy has been employed to deal with the problem of the maximisation of the buckling factor of a VAT multilayer plate subject to both mechanical and manufacturability constraints. On the one hand, the design process is not submitted to restrictions: any parameter characterising the VAT composite (at each scale) is an optimisation variable. This allows the designer to look for a *true global minimum*, hard to be obtained otherwise. On the other hand, both the formulation of the design problem and the MS2L optimisation strategy have been generalised and improved in order to be applied to the problem of designing a VS composite.

In the framework of the MS2L design methodology several modifications have been introduced for both first and second level problems. As discussed in [19], regarding the first-level problem the main modifications are:

- the use of higher-order theories (introduced as result of [29, 30, 31]) for taking into account the influence of the transverse shear stiffness on the overall mechanical response of VAT composites;
- the utilisation of B-spline surfaces for describing the distribution of the laminate polar parameters over the structure which leads to a continuous point-wise variation of the laminate stiffness matrices.

These aspects lead to some important advantages for the resolution of the related optimisation problem. In the most general case the utilisation of B-spline surfaces for describing the point-wise variation of the polar parameters leads to a considerable reduction in the number of design variables (the polar parameters have to be defined solely in each point of the control network of the B-spline surface). In this background, thanks to the *strong convex-hull* property of the B-spline blending functions, the optimisation constraints of the problem (related to the specifications of the considered application) can be imposed only on the control points of the network: if they are satisfied on such points they are automatically met over the whole domain.

In this study a new formalisation of the first-level problem is presented: unlike the approach proposed in [19], only the polar angle $\Phi_1^{A^*}$ varies over the structure (ad its spatial distribution is always described through a B-spline surface), whilst the anisotropic moduli $R_{0K}^{A^*}$ and $R_1^{A^*}$ of the VAT laminate are kept constant. This fact gives rise to some important advantages:

- the feasibility constraints on the laminate polar parameters can be stated only one time for the whole VAT laminate (and not in each point of the control net as in [19]);
- the new formulation of the mechanical design variables allows for integrating the manufacturability requirements linked to the AFP process *since the first step of the strategy* as optimisation constraints on the spatial distribution of the polar angle $\Phi_1^{A^*}$.

The integration of the technological constraints since the first step of the MS2L strategy together with the new formalisation of the first-level problem imply some consequences of paramount importance also for the second-level problem (i.e. the lay-up design of the VAT laminate):

- the fibres-path of each layer can be described through a B-spline surface having the same parameters (number of control points, degree along each direction, components of the knot vectors) of the B-spline surface employed for $\Phi_1^{A^*}$ during the first step of the procedure; moreover the value of the orientation angle at each control point (for each layer) can be got through a straightforward analytical relationship;
- the second-level problem can be formulated and solved only in an arbitrary point of the VAT laminate thus implying a significant reduction of the number of design variables;
- the mathematical formulation of the second-level problem is considerably simplified and it can be stated in the form of an unconstrained minimisation problem (because manufacturability constraints are already included within the first-level problem).

All of these modifications allow to go beyond the main restrictions characterising the design activities and research studies on VAT composites that can be found in literature.

Finally, the effectiveness of the improved version of the MS2L strategy has been proven through a meaningful numerical example. The optimisation tool allows to find an optimum VAT laminate characterised by a significant increment of the first buckling factor (about 78% when manufacturability constraints are not involved and about 67% when they are integrated within the design problem) when compared to a reference classical solution (composed of straight-fibres unidirectional plies).

Concerning the perspectives of this work, there are still some theoretical, numerical and technical aspects that need to be deeply investigated and developed in order to make the proposed approach a very general and comprehensive strategy able to provide solutions that are both efficient (true optimal configurations) and manufacturable. Of course, this action passes through a real understanding of the potential and the technological restrictions linked to the AFP process. Currently, only the technological constraint on the tow steering has been integrated in the MS2L strategy. A step forward can be realised by properly formalising and including into the design problem other kinds of manufacturability constraints: tows gap and overlapping, the variation of the fibre volume fraction due to imperfections, etc. Moreover, from a numerical point of view, the designer could be interested in optimising also the number of design variables (i.e. the number of parameters tuning the shape of the B-spline surfaces) involved into both levels of the MS2L procedure: this point can be easily taken into account by exploiting the original features of the GA BIANCA. Finally, further modifications may also be considered in the formulation of the design problem depending on the nature of the considered application, e.g. by including constraints on inter- and intra-laminar damage, variability effects linked to the fabrication process, costs, etc.

Research is ongoing on all of the previous aspects.

References

[1] Z. Gürdal, B.F. Tatting, and K.C. Wu. Variable stiffness panels: Effects of stiffness variation on the in -plane and buckling responses. *Composites Part A: Applied Science and Manufacturing*, 39(9):11–22, 2008.

[2] M.W. Hyer and H.H. Lee. The use of curvilinear fiber format to improve buckling resistance of composite plates with central circular holes. *Composite Structures*, 18:239–261, 1991.

[3] T.D. Dang and S.R. Hallett. A numerical study on impact and compression after impact behaviour of variable angle tow laminates. *Composite Structures*, 96:194–206, 2013.

[4] G. Raju, Z. Wu, B.C. Kim, and P.M. Weaver. Prebuckling and buckling analysis of variable angle tow plates with general boundary conditions. *Composite Structures*, 94:2961–2970, 2012.

[5] S. Nagendra, S. Kodiyalam, J. Davis, and V. Parthasarathy. Optimization of tow fiber paths for composite design. In *Proceedings of the AIAA/ASME/ASCE/AHS/ASC 36th Structures, Structural Dynamics and Materials Conference*, volume AIAA 95-1275, New Orleans, LA, 1995. American Institute of Aeronautics and Astronautics.

[6] S. Nagendra, D. Jestin, Z. Gürdal, R.T. Haftka, and L.T. Watson. Improved genetic algorithm for the design of stiffened composite panels. *Computers & Structures*, 58(3):543–555, 1996.

[7] M.A. Nik, K. Fayazbakhsh, D. Pasini, and L. Lessard. Surrogate-based multi-objective optimization of a composite laminate with curvilinear fibers. *Composite Structures*, 94:2306–2313, 2012.

[8] M.A. Nik, K. Fayazbakhsh, D. Pasini, and L. Lessard. Optimization of variable stiffness composites with embedded defects induced by automated fiber placement. *Composite Structures*, 107:160–166, 2014.

[9] H. Ghiasi, D. Pasini, and L. Lessard. Optimum stacking sequence design of composite materials Part I: Constant stiffness design. *Composite Structures*, 90:1–11, 2009.

[10] H. Ghiasi, D. Fayazbakhsh, D. Pasini, and L. Lessard. Optimum stacking sequence design of composite materials Part II: Variable stiffness design. *Composite Structures*, 93:1–13, 2010.

[11] M.M. Abdalla, S. Setoodeh, and Z. Gürdal. Design of variable stiffness composite panels for maximum fundamental frequency using lamination parameters. *Composite Structures*, 81:283–291, 2007.

[12] L. Parnas, S. Oral, and U. Ceyhan. Optimum design of composite structures with curved fiber courses. *Composites Science and Technology*, 63:1071–1082, 2003.

[13] S. Setoodeh, M.M. Abdalla, and Z. Gürdal. Design of variable-stiffness laminates using lamination parameters. *Composites: Part B*, 37:301–309, 2006.

[14] S. Setoodeh, M.M. Abdalla, S.T. IJsselmuiden, and Z. Gürdal. Design of variable-stiffness composite panels for maximum buckling load. *Composite Structures*, 87:109–117, 2009.

[15] A.W. Blom, M.M. Abdalla, and Z. Gürdal. Optimization of course locations in fiber-placed panels for general fiber angle distributions. *Composites Science and Technology*, 70:564–570, 2010.

[16] D.M.J. Peeters, S. Hesse, and M.M. Abdalla. Stacking sequence optimisation of variable stiffness laminates with manufacturing constraints. *Composite Structures*, 125:596–604, 2015.

[17] B.C. Kim, P.M. Weaver, and K. Potter. Manufacturing characteristics of the continuous tow shearing method for manufacturing of variable angle tow composites. *Composites: Part A*, 61:141–151, 2014.

[18] B.C. Kim, P.M. Weaver, and K. Potter. Computer aided modelling of variable angle tow composites manufactured by continuous tow shearing. *Composite Structures*, 129:256–267, 2015.

[19] M. Montemurro and A. Catapano. *Variational analysis and aerospace engineering: mathematical challenges for the aerospace of the future*, chapter A new paradigm for the optimum design of variable angle tow laminates. Springer, 2016.

[20] M. Montemurro, A. Vincenti, and P. Vannucci. A two-level procedure for the global optimum design of composite modular structures - application to the design of an aircraft wing. Part 1: theoretical formulation. *Journal of Optimization Theory and Applications*, 155(1):1–23, 2012.

[21] M. Montemurro, A. Vincenti, and P. Vannucci. A two-level procedure for the global optimum design of composite modular structures - application to the design of an aircraft wing. Part 2: numerical aspects and examples. *Journal of Optimization Theory and Applications*, 155(1):24–53, 2012.

[22] A. Catapano and M. Montemurro. A multi-scale approach for the optimum design of sandwich plates with honeycomb core. Part I: homogenisation of core properties. *Composite Structures*, 118:664–676, 2014.

[23] A. Catapano and M. Montemurro. A multi-scale approach for the optimum design of sandwich plates with honeycomb core. Part II: the optimisation strategy. *Composite Structures*, 118:677–690, 2014.

[24] A. Catapano, B. Desmorat, and P. Vannucci. Stiffness and strength optimization of the anisotropy distribution for laminated structures. *Journal of Optimization Theory and Applications*, 167(1):118–146, 2015.

[25] M. Montemurro. *Optimal design of advanced engineering modular systems through a new genetic approach*. PhD thesis, UPMC, Paris VI, France, 2012. http://tel.archives-ouvertes.fr/tel-00955533.

[26] M. Montemurro, A. Vincenti, and P. Vannucci. Design of elastic properties of laminates with minimum number of plies. *Mechanics of Composite Materials*, 48:369–390, 2012.

[27] M. Montemurro, A. Catapano, and D. Doroszewski. A multi-scale approach for the simultaneous shape and material optimisation of sandwich panels with cellular core. *Composites Part B*, 91:458–472, 2016.

[28] G. Verchery. Les invariants des tenseurs d'ordre 4 du type de l'élasticité. VIllard-de-Lans, (France), 1979. Proc. of colloque Euromech 115.

[29] M. Montemurro. An extension of the polar method to the first-order shear deformation theory of laminates. *Composite Structures*, 127:328–339, 2015.

[30] M. Montemurro. Corrigendum to "an extension of the polar method to the first-order shear deformation theory of laminates" [compos. struct. 127 (2015) 328-339]. *Composite Structures*, 131:1143–1144, 2015.

[31] M. Montemurro. The polar analysis of the third-order shear deformation theory of laminates. *Composite Structures*, 131:775–789, 2015.

[32] P. Vannucci. Plane anisotropy by the polar method. *Meccanica*, 40:437–454, 2005.

[33] J. N. Reddy. *Mechanics of composite laminated plates and shells: theory and analysis*. Boca Raton, FL: CRC Press, 2003.

[34] L. Piegl and W. Tiller. *The NURBS Book*. Springer-Verlag, 1997.

[35] P. Vannucci. A note on the elastic and geometric bounds for composite laminates. *Journal of Elasticity*, 112:199–215, 2013.

[36] The MathWorks, Inc., 3 Apple Ill Drive, Natick, MA 01760-2098. *Optimization Toolbox User's Guide*, September 2011.

[37] Ansys. *ANSYS Mechanical APDL Basic Analysis Guide. Release 15.0.* ANSYS, Inc., Southpointe, 275 Technology Drive, Canonsburg, PA 15317, 2013.

[38] P. Vannucci and G. Verchery. A special class of uncoupled and quasi-homogeneous laminates. *Composites Science and Technology*, 61:1465–1473, 2001.

[39] M. Montemurro, A. Vincenti, and P. Vannucci. The automatic dynamic penalisation method (ADP) for handling constraints with genetic algorithms. *Computer Methods in Applied Mechanics and Engineering*, 256:70–87, 2013.

[40] Z. Wu, G. Raju, and P.M. Weaver. Framework for the buckling optimisation of variable-angle-tow composite plates. *AIAA Journal*, 53(12):3788–3804, 2015.

Tables

Technical constants		Polar parameters of [Q] [a]		Polar parameters of $\left[\hat{\mathrm{Q}}\right]$ [b]	
E_1 [MPa]	161000.0	T_0 [MPa]	23793.3868	T [MPa]	5095.4545
E_2 [MPa]	9000.0	T_1 [MPa]	21917.8249	R [MPa]	1004.5454
G_{12} [MPa]	6100.0	R_0 [MPa]	17693.3868	Φ [deg]	90.0
ν_{12}	0.26	R_1 [MPa]	19072.0711		
ν_{23}	0.10	Φ_0 [deg]	0.0		
		Φ_1 [deg]	0.0		
Density and thickness					
ρ [Kg/mm^3]	1.58×10^{-6}				
h_{ply} [mm]	0.125				

[a] In-plane reduced stiffness matrix of the pre-preg strip.
[b] Out-of-plane shear stiffness matrix of the pre-preg strip.

Table 1: Material properties of the carbon-epoxy pre-preg strip taken from [29, 30].

Sides	BCs
AB, CD	$U_x = 0$
	$U_z = 0$
BC, DA	$U_y = 0$
	$U_z = 0$

Table 2: BCs of the FE model of the VAT laminated plate.

Design variable	Type	Lower bound	Upper bound
R_{0K}^{A*} [MPa]	continuous	-17693.3868	17693.3868
R_1^{A*} [MPa]	continuous	0.0	19072.0711
$\Phi_1^{A*(i,j)}$ [deg]	continuous	-90.0	90.0

Table 3: Design space of the first-level problem.

Genetic parameters		
	1^{st} level problem	2^{nd} level problem
N. of populations	1	1
N. of individuals	270	500
N. of generations	250	500
Crossover probability	0.85	0.85
Mutation probability	0.0037	0.002
Selection operator	roulette-wheel	roulette-wheel
Elitism operator	active	active

Table 4: Genetic parameters of the GA BIANCA for both first and second-level problems.

Polar parameters		
	case 1	case 2
${R_{0K}}^{A^*}$	13756.4634	−17693.3868
${R_1}^{A^*}$	17164.86	0.0000

Table 5: Optimum value of the polar parameters ${R_{0K}}^{A^*}$ and ${R_1}^{A^*}$.

n_p \ m_p	0	1	2	3	4
0	−45.5311	−10.1854	−85.8024	90.0000	−60.6225
1	−59.4246	−90.0000	90.0000	71.8029	81.9769
2	−70.5450	39.6424	−90.0000	−48.3263	0.2430
3	87.7414	55.5200	71.4718	−77.6823	−42.7740
4	−58.0815	90.0000	−1.2187	−78.7346	−31.8303

Table 6: Optimum value of ${\Phi_1}^{A^*}$ [deg] for each control point of the B-spline surface, case 1.

n_p \ m_p	0	1	2	3	4
0	49.1349	40.1612	54.0772	30.9143	44.3536
1	33.0933	86.2196	40.7661	15.8884	60.8939
2	29.1137	21.5929	51.7663	47.8135	59.6959
3	66.0686	29.2392	54.6419	55.1906	28.4075
4	40.2953	25.9924	41.6383	71.7229	45.2671

Table 7: Optimum value of ${\Phi_0}^{A^*}$ [deg] for each control point of the B-spline surface, case 2.

n_p \ m_p	0	1	2	3	4
0	−45.2978	−9.9521	−85.5691	90.2333	−60.3892
1	−59.1913	−89.7667	90.2333	72.0362	82.2102
2	−70.3117	39.8757	−89.7667	−48.0930	0.4763
3	87.9747	55.7533	71.7051	−77.4490	−42.5407
4	−57.8482	90.2333	−0.9854	−78.5013	−31.5970

Table 8: Optimum value of ${\delta_0}^{(i,j)}$ [deg] for each control point of the B-spline surface of the 1^{st} saturated group, case 1.

n_p \ m_p	0	1	2	3	4
0	−60.2978	−24.9521	−100.5691	75.2333	−75.3892
1	−74.1913	−104.7667	75.2333	57.0362	67.2102
2	−85.3117	24.8757	−104.7667	−63.0930	−14.5237
3	72.9747	40.7533	56.7051	−92.4490	−57.5407
4	−72.8482	75.2333	−15.9854	−93.5013	−46.5970

Table 9: Optimum value of ${\delta_1}^{(i,j)}$ [deg] for each control point of the B-spline surface of the 2^{nd} saturated group, case 1.

n_p \ m_p	0	1	2	3	4
0	−31.2978	4.0479	−71.5691	104.2333	−46.3892
1	−45.1913	−75.7667	104.2333	86.0362	96.2102
2	−56.3117	53.8757	−75.7667	−34.0930	14.4763
3	101.9747	69.7533	85.7051	−63.4490	−28.5407
4	−43.8482	104.2333	13.0146	−64.5013	−17.5970

Table 10: Optimum value of ${\delta_2}^{(i,j)}$ [deg] for each control point of the B-spline surface of the 3^{rd} saturated group, case 1.

n_p \ m_p	0	1	2	3	4
0	49.1349	40.1612	54.0772	30.9143	44.3536
1	33.0933	86.2196	40.7661	15.8884	60.8939
2	29.1137	21.5929	51.7663	47.8135	59.6959
3	66.0686	29.2392	54.6419	55.1906	28.4075
4	40.2953	25.9924	41.6383	71.7229	45.2671

Table 11: Optimum value of ${\delta_0}^{(i,j)}$ [deg] for each control point of the B-spline surface of the 1^{st} saturated group, case 2.

n_p \ m_p	0	1	2	3	4
0	−40.8651	−49.8388	−35.9228	−59.0857	−45.6464
1	−56.9067	−3.7804	−49.2339	−74.1116	−29.1061
2	−60.8863	−68.4071	−38.2337	−42.1865	−30.3041
3	−23.9314	−60.7608	−35.3581	−34.8094	−61.5925
4	−49.7047	−64.0076	−48.3617	−18.2771	−44.7329

Table 12: Optimum value of ${\delta_2}^{(i,j)}$ [deg] for each control point of the B-spline surface of the 2^{nd} saturated group, case 2.

Figures

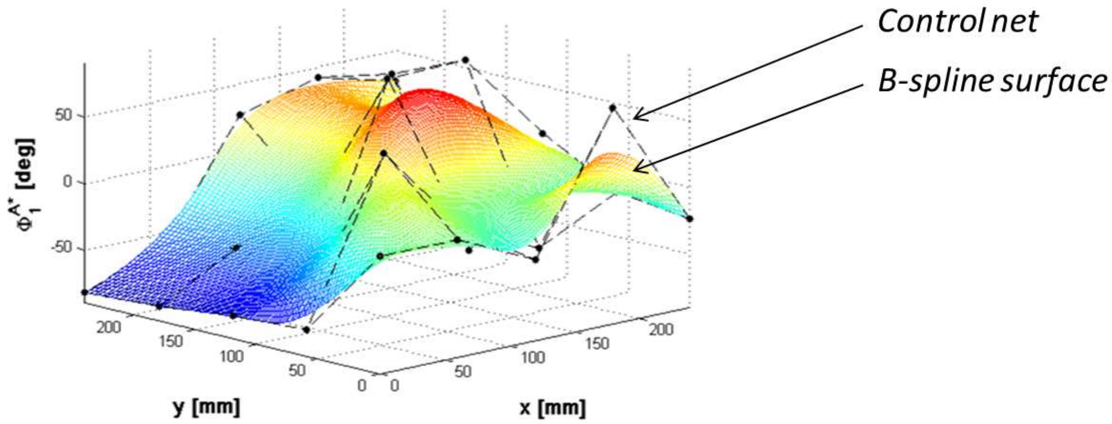

Figure 1: Example of a B-spline surface representing the spatial distribution of ${\Phi_1}^{A^*}$.

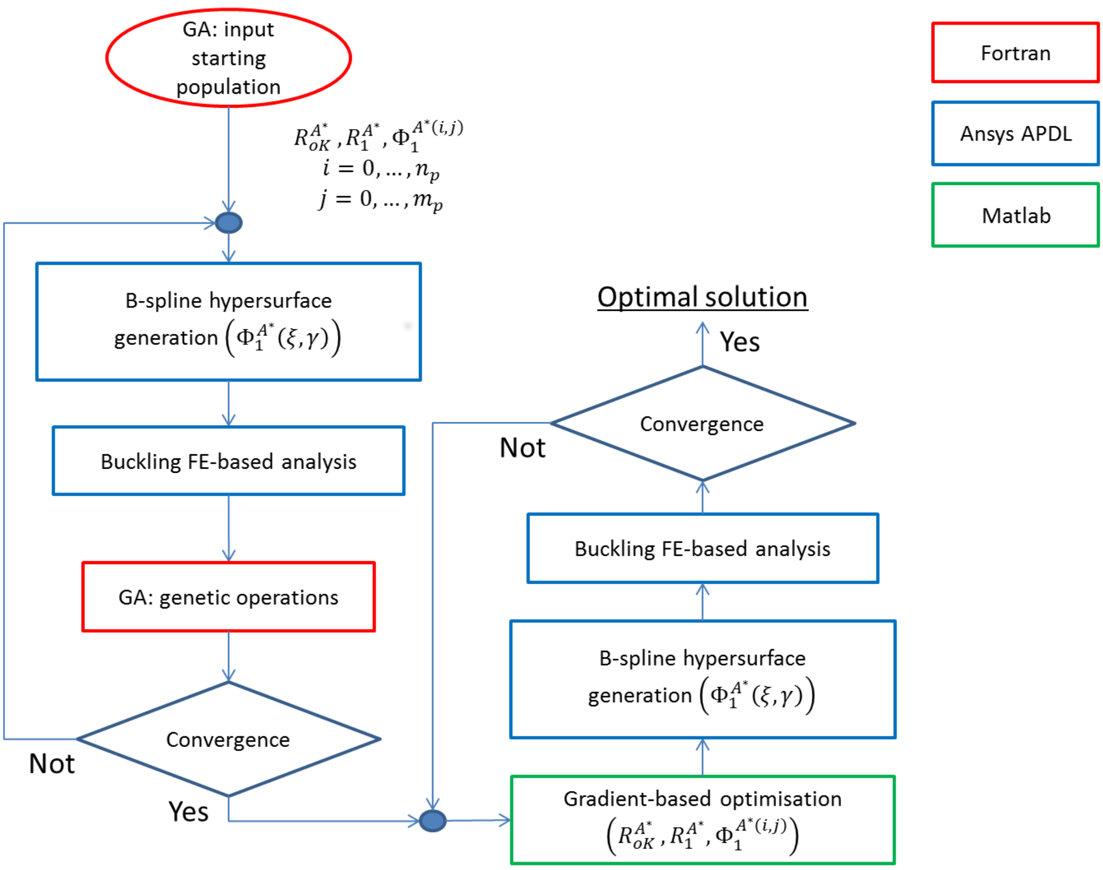

Figure 2: Logical flow of the numerical procedure employed for the solution search of the first-level problem.

Fixed chromosome	R_{0K}^{A*}	R_1^{A*}
Modular part: $(n_p + 1) \times (m_p+1)$ chromosomes	$\phi_1^{A*(0,0)}$	
	$\phi_1^{A*(1,0)}$	
	...	
	$\phi_1^{A*(n_p,m_p-1)}$	
	$\phi_1^{A*(n_p,m_p)}$	

Figure 3: Structure of the genotype of the generic individual for problem (14).

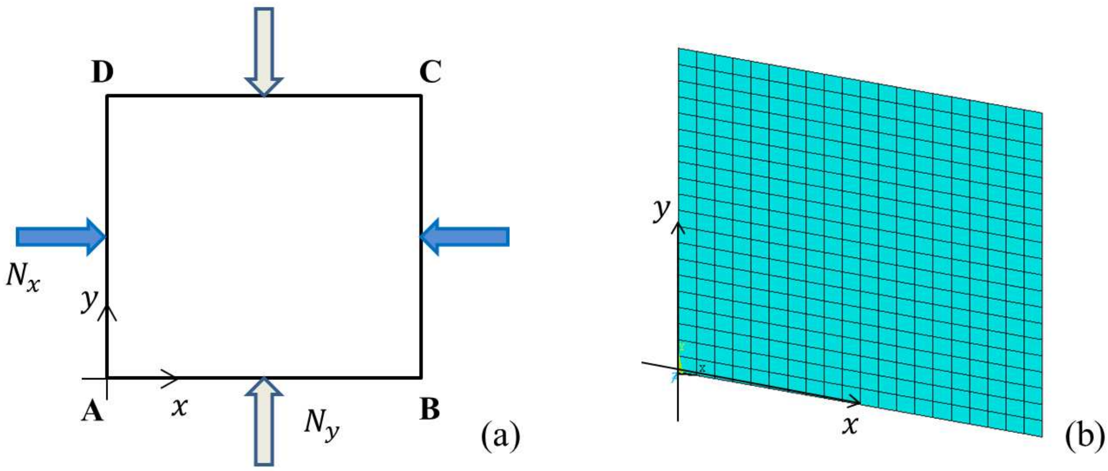

Figure 4: Geometry of the VAT plate: applied BCs (a) and FE model of the structure (b).

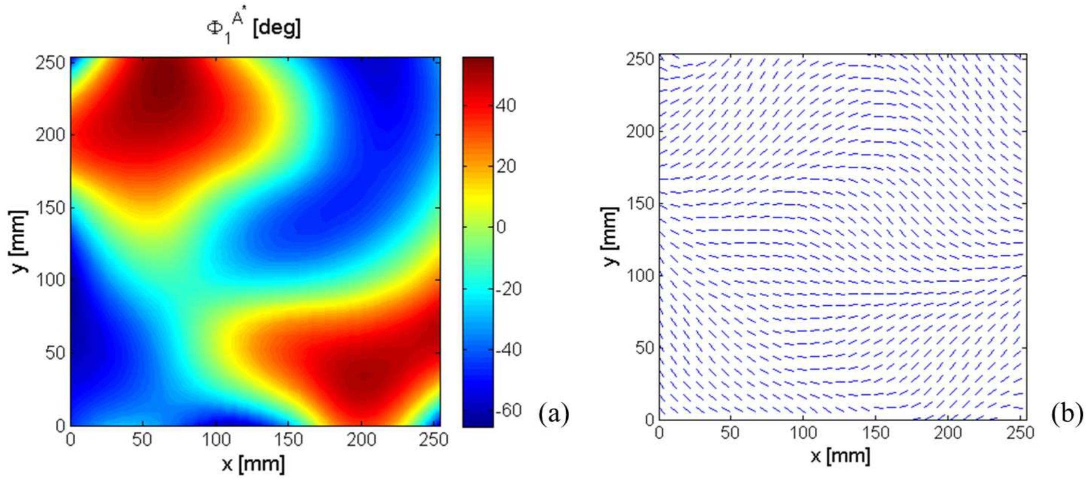

Figure 5: Optimal distribution of the polar angle ${\Phi_1}^{A^*}$ over the VAT plate resulting from the first-level optimisation problem, contour plot (a) and quiver plot (b), case 1.

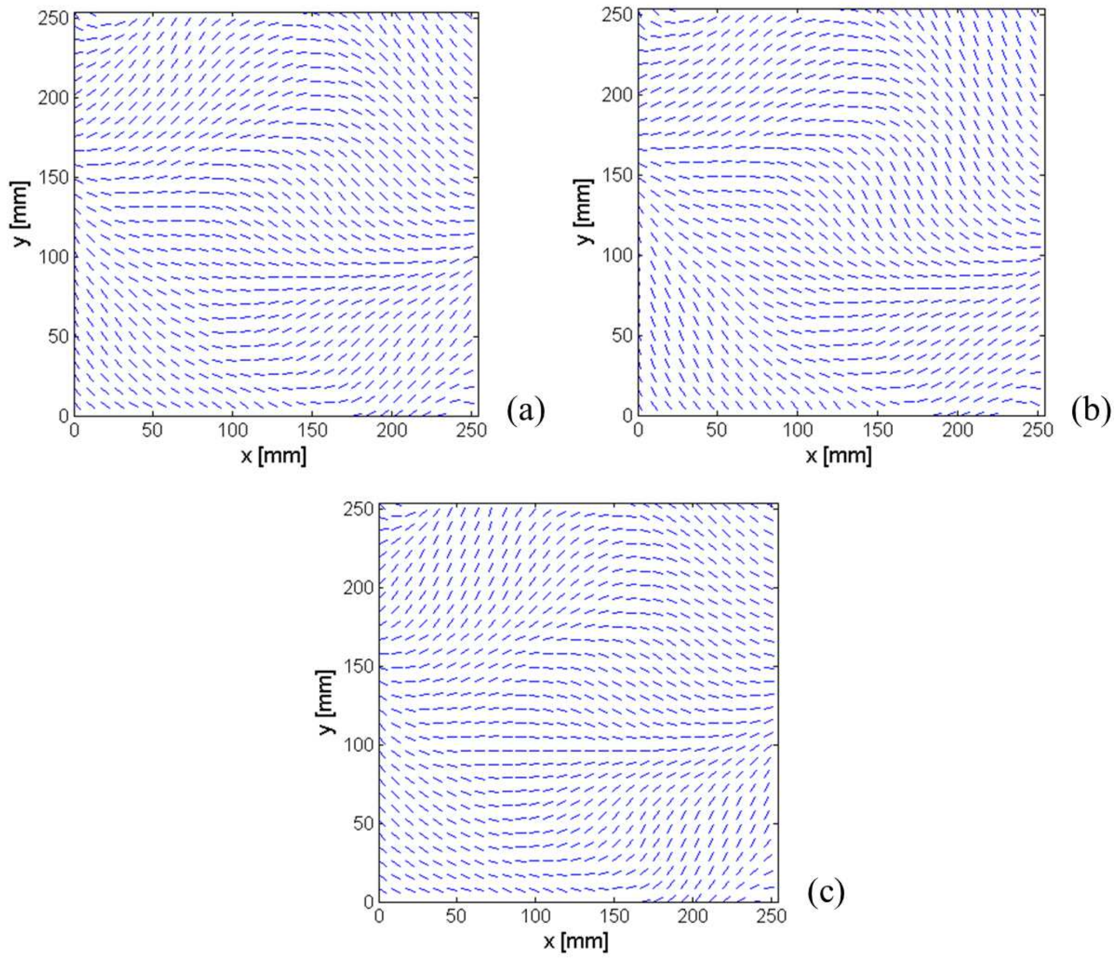

Figure 6: Optimum fibres path for the three groups of layers of the VAT plate resulting from the second-level optimisation problem, 1^{st} group (a), 2^{nd} group (b) and 3^{rd} group (c), case 1.

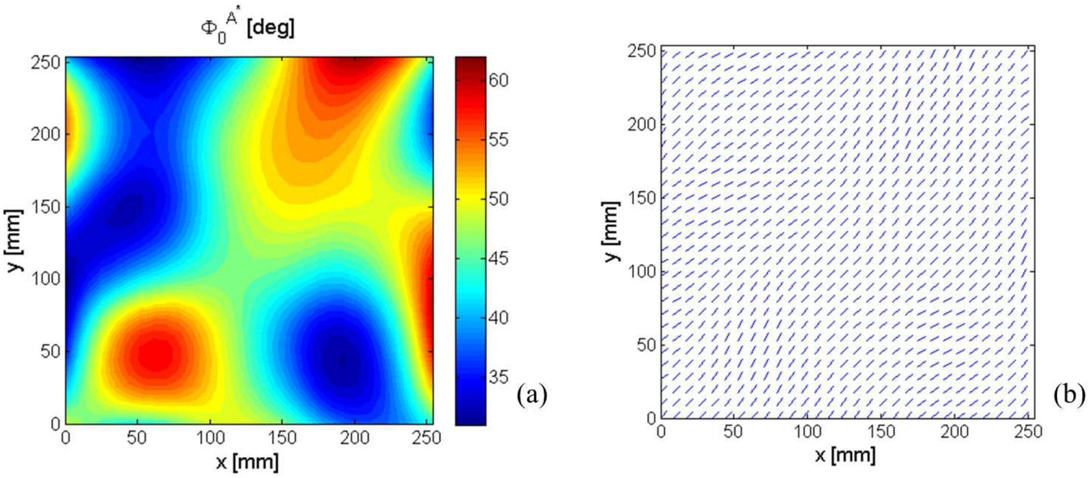

Figure 7: Optimal distribution of the polar angle ${\Phi_0}^{A^*}$ over the VAT plate resulting from the first-level optimisation problem, contour plot (a) and quiver plot (b), case 2.

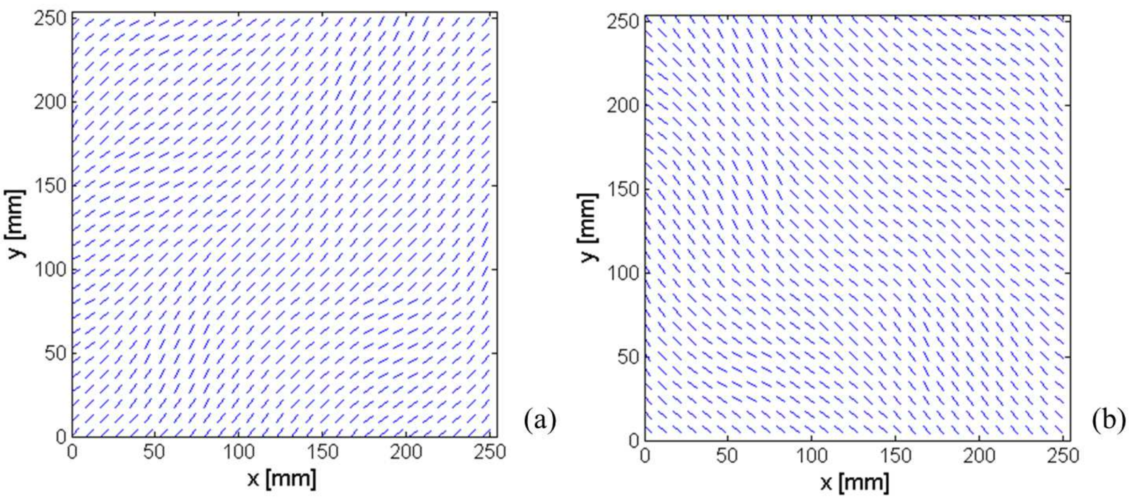

Figure 8: Optimum fibres path for the two groups of layers of the VAT plate resulting from the second-level optimisation problem, 1^{st} group (a) and 2^{nd} group (b), case 2.